Science of the Total Environment 543 (2016) 357–372

Contents lists available at ScienceDirect

Science of the Total Environment

journal homepage: www.elsevier.com/locate/scitotenv

Hydrogeochemical signatures and evolution of groundwater impacted by the Bayan Obo tailing pond in northwest China

Xiang Huang [a,b], Hailin Deng [c,*], Chunmiao Zheng [a,d,e], Guoliang Cao [a]

[a] Institute of Water Sciences and College of Engineering, Peking University, Beijing, China
[b] Shaanxi Key Laboratory of Comprehensive Utilization of Tailing Resources, Shangluo University, Shaanxi, China
[c] CSIRO Land and Water, Private Bag No. 5, Wembley, WA 6913, Australia
[d] School of Environmental Science and Engineering, South University of Science and Technology of China, Shenzhen, China
[e] Department of Geological Science, University of Alabama, Tuscaloosa, AL, USA

HIGHLIGHTS

- Combining hydrogeochemical methods and multivariate statistical analysis.
- First reporting geochemical processes in aquifers nearby Bayan Obo REE tailing pond.
- No geochemical evidence for uranium and thorium contamination in shallow groundwater.

GRAPHICAL ABSTRACT

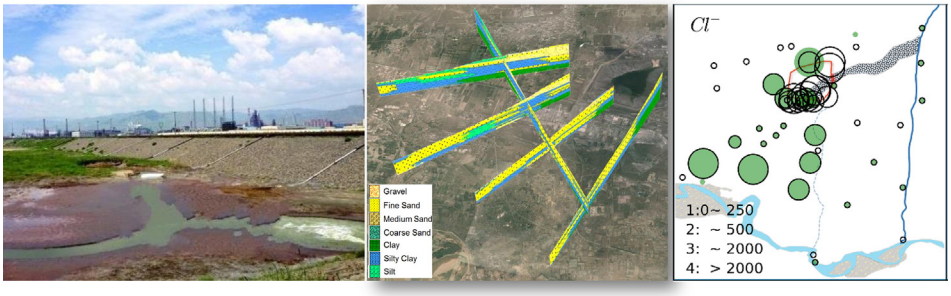

ARTICLE INFO

Article history:
Received 28 September 2015
Received in revised form 29 October 2015
Accepted 29 October 2015
Available online xxxx

Editor: D. Barcelo

Keywords:
Hydrogeochemistry
Groundwater
Multivariate statistical analysis
Tailing pond leakage
Bayan Obo

ABSTRACT

Uncontrolled leakage from mine tailing ponds can pose a serious environmental threat. Groundwater quality in a semi-arid region with extensive worries about the leakage from one of world's largest tailing ponds is studied herein through an integrated hydrogeochemical analysis and multivariate statistical analysis. Results show that elevated concentrations of NO_2^-, B, Mn, NH_4^+, F^-, and SO_4^{2-} in groundwater were probably caused by leakage from the tailing pond and transported with the regional groundwater flow towards downstream Yellow River. While NO_2^- contamination is only limited to areas close to the pond, high B concentrations persist within the contaminated plume originating from the tailing pond. Our current study shows that there is no geochemical evidence for U and Th contamination in groundwater due to leakage from the Bayan Obo tailing pond. Combining effects which includes regional variations, pond leaking and downstream mixing, mineral precipitation and dissolution, redox processes, ion exchange processes and agricultural activities, controlled groundwater hydrogeochemical signatures in the studied area. This study demonstrate that an increase in knowledge of evolution of groundwater quality by integrating field hydrochemical data and multivariate statistical analysis will help understand major water–rock interactions and provide a scientific basis for protection and rational utilization of groundwater resources in this and other tailing-impacted areas.

* Corresponding author.
E-mail address: hailin.deng@gmail.com (H. Deng).

http://dx.doi.org/10.1016/j.scitotenv.2015.10.150
0048-9697/

1. Introduction

Mine tailings are often stored in pond behind dams, which often pose serious threat to surrounding environment because of potential dam failure, seepage of potential hazardous contaminants, negative visual impacts and damage of substrate bearing capacity (e.g., Johnson and Hallberg, 2005; Wolkersdorfer, 2008; Pan, 2010). Many tailing sites are historically adjacent to water bodies and immediately surrounded by industrial and agricultural areas (e.g., Penman, 2001; Olías et al., 2004; Pan, 2010). However, the impacts of these tailing ponds on nearby groundwater quality were not well studied or reported probably because of no routine monitoring and few complete hydrogeochemical data. There are not such many examples as mine sites in the Odiel River basin (e.g., Olías et al., 2004), the Old Rifle site and Hanford site (e.g., Zachara et al., 2013), where contaminated groundwater was studied in details. While significant efforts have been made to understand the behavior and fate of leachate plumes emanating from unlined tailing ponds or ponds with ruptured liners at their base as well as pit lakes (e.g., Johnson and Hallberg, 2005; Pan, 2010), groundwater quality impacted by above-ground tailing ponds has rarely been well documented. The high elevation of the above-ground tailing pond, which generates relatively high hydraulic gradient, causes its leaking events and the associated impacts on the groundwater system, which are not only limited to immediately downstream areas of the pond, but extended to farther areas.

A growing environmental awareness in China has led to increasing concerns for the risks from dam failures and waste disposal management associated with mining activities (e.g., Pan, 2010; Guo and Tong, 2011; Zhang, 2013). Based on data compiled in China in 2009, there were 26,000 registered tailing ponds while 300 new ponds were being constructed on average each year (Shen et al., 2011). So far, however, very few studies have comprehensively investigated the impacts of leakage of tailing ponds, identified characteristic hydrochemical changes in the surrounding aquifers and further determined whether groundwater quality has been deteriorated. The Bayan Obo (Baiyun Erbo or Baotou) tailing pond, known as the largest rare earth elements (REE) tailing pond in the world (e.g., Yu et al., 2012; Hurst, 2010; Huang et al., 2014), has received large volumes of tailings from the Baogang flotation-hydrometallurgical processing plant since the 1960s. The Baogang processing plant smelts ores which are extracted from the giant Bayan Obo deposit. At the earlier years of its operation, eco-environmental risks were not comprehensively examined and the pond was constructed as an "artificial lake" without full pre-cautions to protect the surrounding environment. More recently, however, with increasing pond levels in conjunction with rising environmental awareness, the Bayan Obo tailing pond has received an urgent-extensive call to comprehensively study and initiate remediation of the site, if deemed necessary (e.g., Xu et al., 2005; Guo and Tong, 2011; Huang, 2011). The major concerns are driven by the potential threat to the downgradient Yellow River, which is the primary water source for approx. 150 million people. Some sparse data regarding the surrounding hydrogeology were collected and reported by Shen and Liu (1957); Zhu (1962), and Fang (2006), and other limited groundwater quality data were reported by Zheng and Lu (1986) and Wang and Tu (1990). Also, recently Liao (2013) developed a regional flow model to investigate strategies for a sustainable development of groundwater resources in Baotou City, without considering hydraulic impacts from that tailing pond. The most comprehensive overview of previous activities was recently contributed by Huang et al. (2014), who summarized the sparse historical data with a systematic review on leachate and their background concentrations in groundwater. Their study suggested that uncaptured leakages had resulted in a plume of pervasively contaminants that extended in southwestward direction towards the downstream fluvio-lacustrine aquifer, and had probably reached the Yellow River alluvium plain and its contiguous swamps.

In this study, integrating existing and our new data, we use a range of techniques to elucidate what processes control the hydrogeochemical evolution of the groundwater system between the tailing ponds and the Yellow River. Principle component analysis (PCA) and Hierarchical cluster analysis (HCA) were used to constrain the relationships among groundwater constituents. The overall objective of this study is to identify whether, and if, to what degree leakage from the Bayan Obo tailing pond and other anthropogenic sources have contaminated the shallow aquifer system and the Yellow River, and what risks this may pose at present and in future. Therefore, this study will provide essential guidance for the future management of the groundwater systems and remediation requirements, while also guiding future monitoring activities.

2. Material and methods

2.1. Hydrogeological setting

The study area is located in the Yellow River alluvial plain near the piedmont of the Daqingshan Mountains, which also belongs to the western part of the Hubao plain in northwest China. The northern Daqingshan–Wulashan piedmont fault and southern Lana fault divide this region into the piedmont clinoplain and the Yellow River alluvial plain (Wang, 2006). The piedmont region of the Daqingshan–Wulashan Mountains is a groundwater recharge zone which is mainly composed of pre-Cambrian fractured metamorphic rock while the down gradient piedmont clinoplain and alluvial plain are mostly characterized by Quaternary unconsolidated sediments (Wang, 2006) that host rather transmissive, saturated aquifers. The Quaternary unconsolidated sediments consisting of coarse alluvial gravels and pebbles are extensively interlayered within three major alluvial–pluvial fans (Shen and liu, 1957), i.e., the Hademen ravine, Kundulun River and Dongdaben gully in the north (Fig. 1). In the northern piedmont clinoplain (average elevation of 1080 m), which is characterized by an average slope gradient of 8%, a formation of substantial fractions of clayey sand mixed with gravel forms a high-yielding aquifer. The southern Yellow River alluvial plain is relatively flat with an average elevation of 1010 m and a slope gradient ranging from 0.1 to 1.0%, associated with small hydraulic gradients. Representative hydrogeological cross-sections are shown in Fig. 2. They depict the major geological layers in the vicinity of the pond. The sequence shown in Fig. 2 also includes a thick impermeable unit of Pleistocene–Holocene muddy clays, which acts as a broadly distributed confining layer between the deep confined and the shallow unconfined aquifers (Zhu, 1962; Zheng and Lu, 1986; Fang, 2006). The thickness of the shallow aquifer is generally 25 - 35 m. In the upgradient of the southern Yellow River alluvial plain, the shallow aquifer is mainly composed of gravel and pebbles. In the downgradient areas contiguous to the Yellow River, there are massive interbeds of fluviolacustrine sediments in the shallow aquifer. These detrital sediments mainly consist of silt, clayey silt, silty sand and clay, which were generated from earlier swamps and wetlands (Zhu, 1962; Fang, 2006).

A temperate climate with East Asian continental monsoon predominates in this arid to semi-arid area. The long-term annual rainfall is in the range of 175 to 400 mm with 2100 to 2700 mm of evaporation and more than 75% of the rainfall occurs between May and September (Supporting information Fig. S1) (Fang, 2006). The groundwater levels in the shallow aquifer varied from 1.2 to 6.6 m below ground level in 2013 and were generally higher in July 2013 (wet season) than in November 2013 (dry season). The amplitude of the seasonal variations in the water table was found to range between 0.1 and 1.5 m. The hydraulic gradient varied by approximately 0.5% regionally, but close to the tailing pond, it is locally higher, especially near the leachate collection trench and near the Baolan railway dyke (Fig. 1). For example, several local groundwater mounding (or spring) zones/points have continuously been observed nearby the railway dyke and trench. In areas below and around the pond, both the magnitude and the

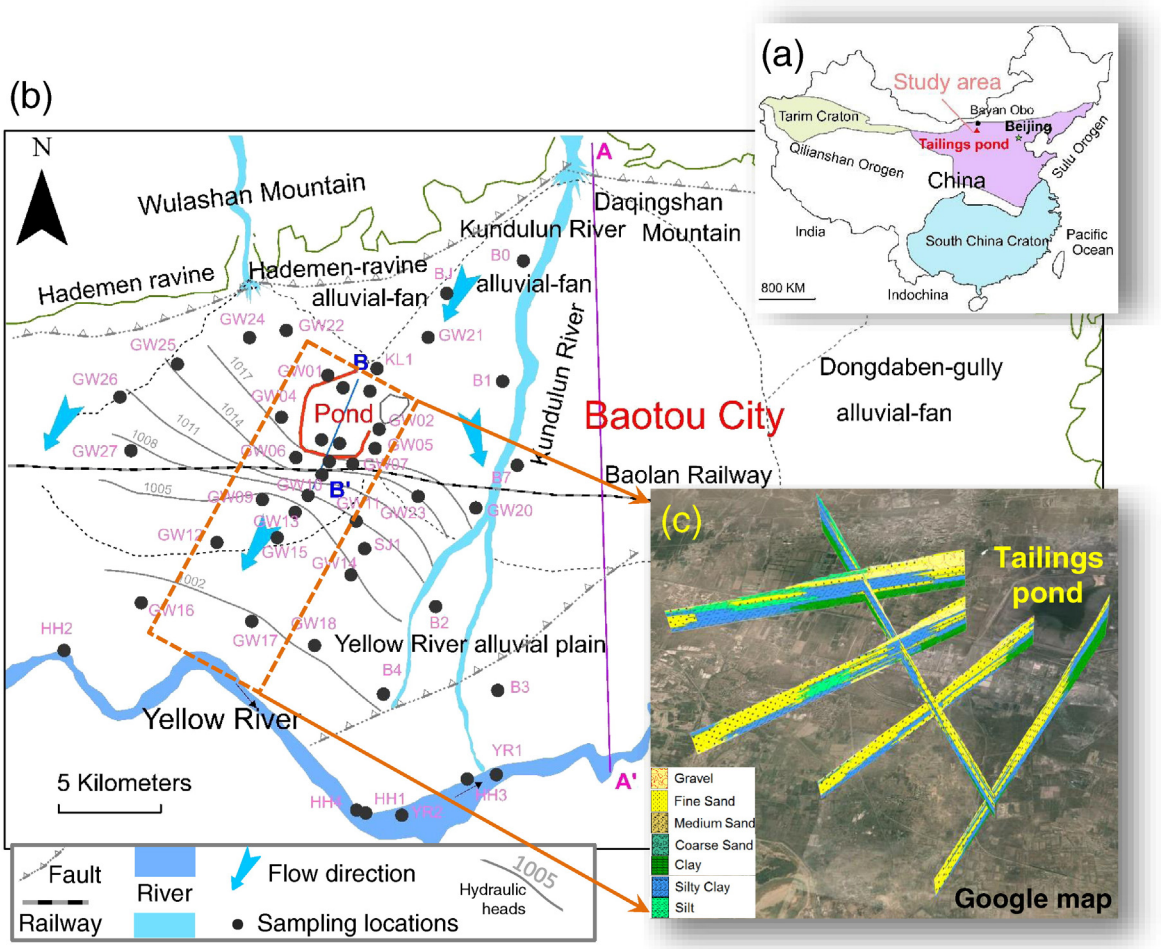

Fig. 1. (a) Simplified map showing the location of the Bayan Obo deposit and its tailings, modified from Yang et al. (2011). (b) Sketched geological map of the Bayan Obo tailing pond and its hydrogeological setting, modified after Zhu (1962); Zheng and Lu (1986); (c) 3D fence diagram of stratigraphy was constructed by the ArcGIS interpolating 65 bore logs (ca. 35 m in shallow aquifer) and then was projected on a Google map. Transects A–A′ and B–B′ are interpreted in Fig. 2. The regional groundwater flow is from northeast to southwest, which are generally oriented perpendicular to the equipotential lines of hydraulic heads (Kriging interpolated based on field measurements in 2013 July).

direction of the hydraulic gradient are very likely to differ from the regional gradient because this old pond with high elevations is situated in the juncture of several alluvial-fans, which results in relatively complex hydrogeological characteristics. Hydraulic conductivities were retrieved from pumping tests in the field ranging from 2 to 50 m/day. Seasonal infiltration from precipitation and irrigation return flows might locally affect flow regimes in the downgradient regions in the vicinity of the Yellow River. Historically, in this area variation between dry and wet period caused frequent problems related to ephemeral flooding, water logging and drainage congestion during the monsoon season (Zheng, 1992; Fang, 2006). With the exception of flood periods, groundwater mainly discharges to the Yellow River. However, the shallow aquifer can locally be directly recharged by the fluctuating river water during wet seasons.

2.2. Characteristics of tailing pond and waste disposal

Since 1965 the Bayan Obo tailing pond has been used to store REE-enriched tailings derived from the smelting and refining processes during development of the Bayan Obo REE–Nb–Fe deposit. The carbonate-hosted Bayan Obo ore, situated in the semi-arid steppe at the north margin of the North China Craton, is known as the world's largest REE deposit, mainly enriched in monazite and bastnaesite (Huang, 2011; Yu et al., 2012; Ma, 2012). Earlier studies on the Bayan Obo type deposit are documented in Guo (1989); Yang et al. (2011); Yu et al. (2012) and Ma (2012). Compared with other single bastnaesite ores, the Bayan Obo ore is significantly more difficult to refine owing to its physical and chemical properties being similar to gangue minerals (Huang, 2011). Additional processing/extraction and refining in multiple steps are required before extracting REEs. These processing typically produce large amounts of CO_2 and fluoride after calcining bastnaesite and using concentrated sulfuric acid (Huang, 2011). It is then hydrometallurgically treated by two main digestions stages with hydrochloric acid, and further treated with precipitating agents [$(NH_4)HCO_3$ and/or NaOH] to produce rare earth hydroxides (REOs) (Huang, 2011; Ma, 2012). Briefly, such extraction processes typically involve the large use of sulfuric, hydrochloric and hydrofluoric acids, and the following successive solvent extraction–precipitation steps consume considerable quantities of oxalic acid ($C_2H_2O_4$) and/or ammonium bicarbonate [$(NH_4)\ HCO_3$]. Finally, most of processing waste water and slurries were disposed into the Bayan Obo tailing pond, from which it could potentially leak into surrounding water bodies.

The tailing dam has been raised by the center-line method of construction using an 11.5-km-long dyke with maximum 35-m-height above its foundation and currently form an effective storage capacity

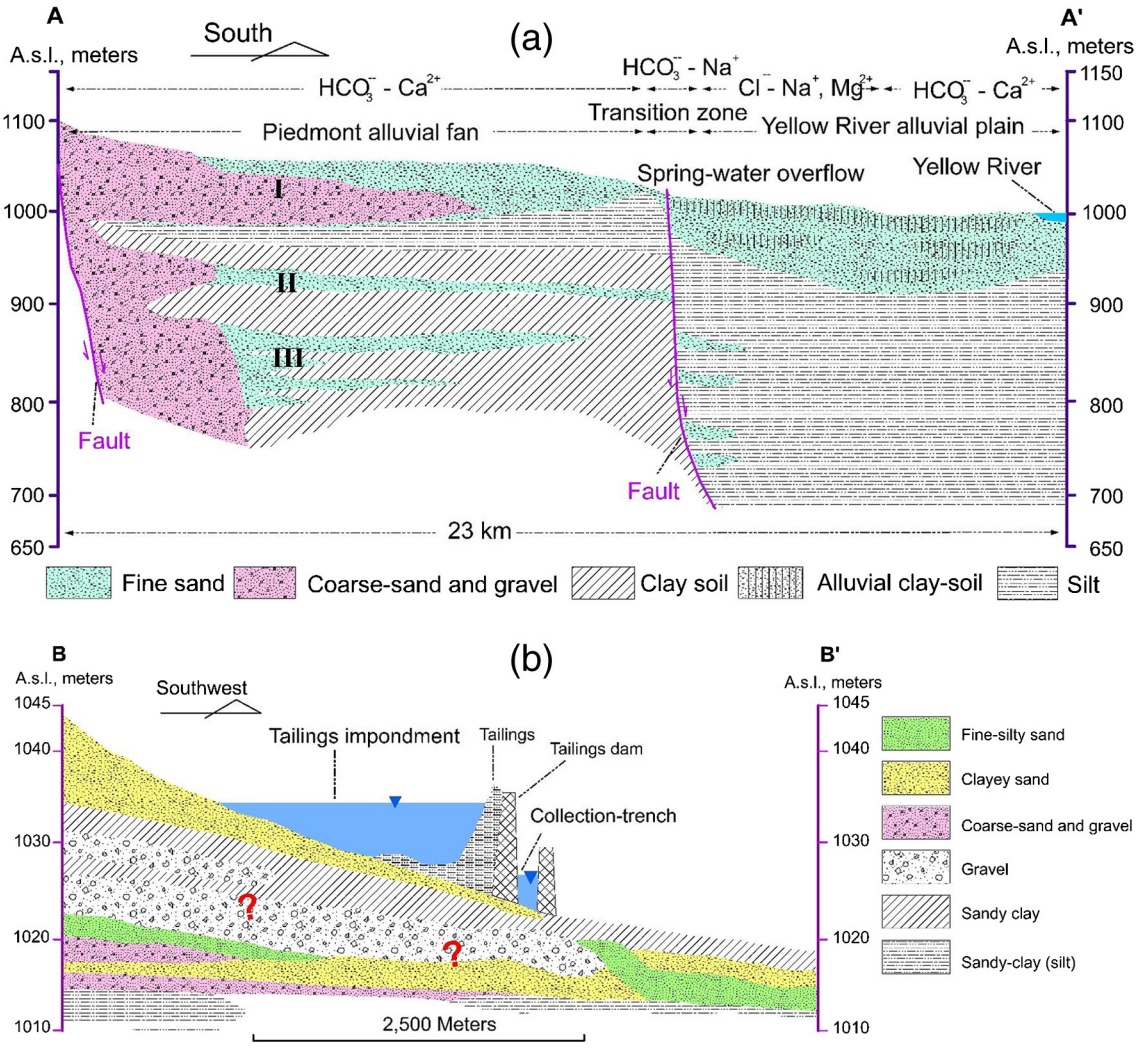

Fig. 2. Two representative hydrogeological cross sections A–A′ and B–B′, shown in Fig. 1b. (a) Aquifer unit I correspond to the shallow aquifer in this study, and deep aquifers refer to aquifer units II and III; hydrochemical types and geomorphic features are compiled from Zheng (1992). (b) One transect across the tailing pond modified from Zheng and Lu (1986).

of 70 million m^3. Similar to other tailing sites in the early phases of mining in China and many other countries, either no or only a poorly resistive bottom liner with/without engineered cover was used to prevent leaching from the pond. The tailing dam is barren of vegetation and has a poor aggregate structure. As a consequence, it is susceptible to erosion by wind and water. Additionally, increasing industrial activities and agricultural practices have changed land-use greatly since 1970s (Supporting information Fig. S2). In the vicinity of the tailing pond, agricultural lands and local surface water bodies have been reported to be heavily contaminated (Wang and Tu, 1990; Pan, 2010). Because of its high elevation and storing collection of a substantial amount of radioactive thorium and uranium and daughter radionuclides (Liu, 2011; Huang et al., 2014; Ma, 2012), Xu et al. (2005) and Ma (2012) expressed urgent concerns about the potential radioactive threat to the downstream Yellow River and the large risk of dam failure. Furthermore, a strong earthquake of M 6.4 occurred in this area in 1996 (Nie et al., 2011). All these have rendered the tailing pond infamous as a "suspended radioactive lake".

2.3. Water sampling and analysis

Based on the comprehensive analysis of the geologic and hydrogeological conditions and earlier investigations of groundwater, soil and dust in the surroundings of the Bayan Obo tailing pond (e.g., Wang and Tu, 1990; Xu et al., 2005; Si et al., 2015; Huang et al., 2014), 66 samples were collected from 49 groundwater and 17 surface water sites in July and November 2013. The locations of the sampling sites are shown in Fig. 1. The surface water group, including three swamp water samples, four leachate collection-trench water samples, one slurry water sample and six river water samples, were collected at depth from 0.2 to 0.5 m below the water table. Eighteen groundwater samples were collected from newly drilled monitoring wells at an average depth of 30 m and the rest from nearby production wells at depth of approximately 40 m. The leachate sample (or pore water) was collected through a drive-in piezometer and inertial pump at a depth of 1.2 m below the dry beach in the tailing pond, which was grouped into groundwater in the following analysis.

Before taking groundwater samples at least three well casing volumes were pumped until the field parameters stabilized, as measured in a small flow-through chamber following the procedure described by Wolkersdorfer (2008). After sampling all field parameters were recorded using a multi-parameter portable meter (WTW3230i®). All water samples were filtered (0.45 μm, regenerated cellulose) and then stored at 4 °C in darkness prior to analysis. Alkalinity was determined in triplicate on filtered samples in the field and/or during the sampling day by titration with H_2SO_4 (0.22 N). High-density polyethylene sample

containers were pre-washed with 5% super-pure HCl and then triple-rinsed with deionized water (RO-DI600) before being brought to sampling in the field. Each sample bottle was rinsed three times before being filled. Samples for cation analyses were acidified to pH < 2 with super-pure nitric acid (HNO_3). Filtered, non-acidified samples were used for analysis of anions. Major anions and cations were determined using ion chromatography (Dionex-500, precision ±5–10%), while minor/trace elements were determined using ICP-OES (PerkinElmer, 5300DV) and ICP-MS (2000E) at the Analytical Laboratory in the Beijing Research Institute of Uranium Geology (ALBRIUG). Several parameters, such as CODmn (an aggregative pollution indicator contributed by organic and reducing inorganic matter), NO_3^--N, NO_2^--N, NH_4^+-N, F^-, As, Hg, Cr and Se, were reanalyzed at the Baotou Environmental Monitoring Center. All analyses were performed as triplicates (Wolkersdorfer, 2008) and measurement errors showed to be ≤5% for all samples. Quality assurance/quality control (QA/QC) procedures were used in all the processes from the field to the final lab analysis.

The geochemical modeling program PHREEQC (Parkhurst and Appelo, 1999) was used to calculate speciation distribution and saturation indices of major mineral phases (e.g., calcite, dolomite, siderite, gypsum, anhydrite, fluorite, quartz and halite) under thermodynamic equilibrium with respect to the theoretical partial pressure of CO_2 in water.

2.4. Statistical analysis

Multivariate statistical methods have been widely used to analyze groundwater hydrogeochemical data to attain meaningful relationships among the investigated variables (e.g., Merchán et al., 2015; Biswas et al., 2012). Principal component analysis (PCA), hierarchical cluster

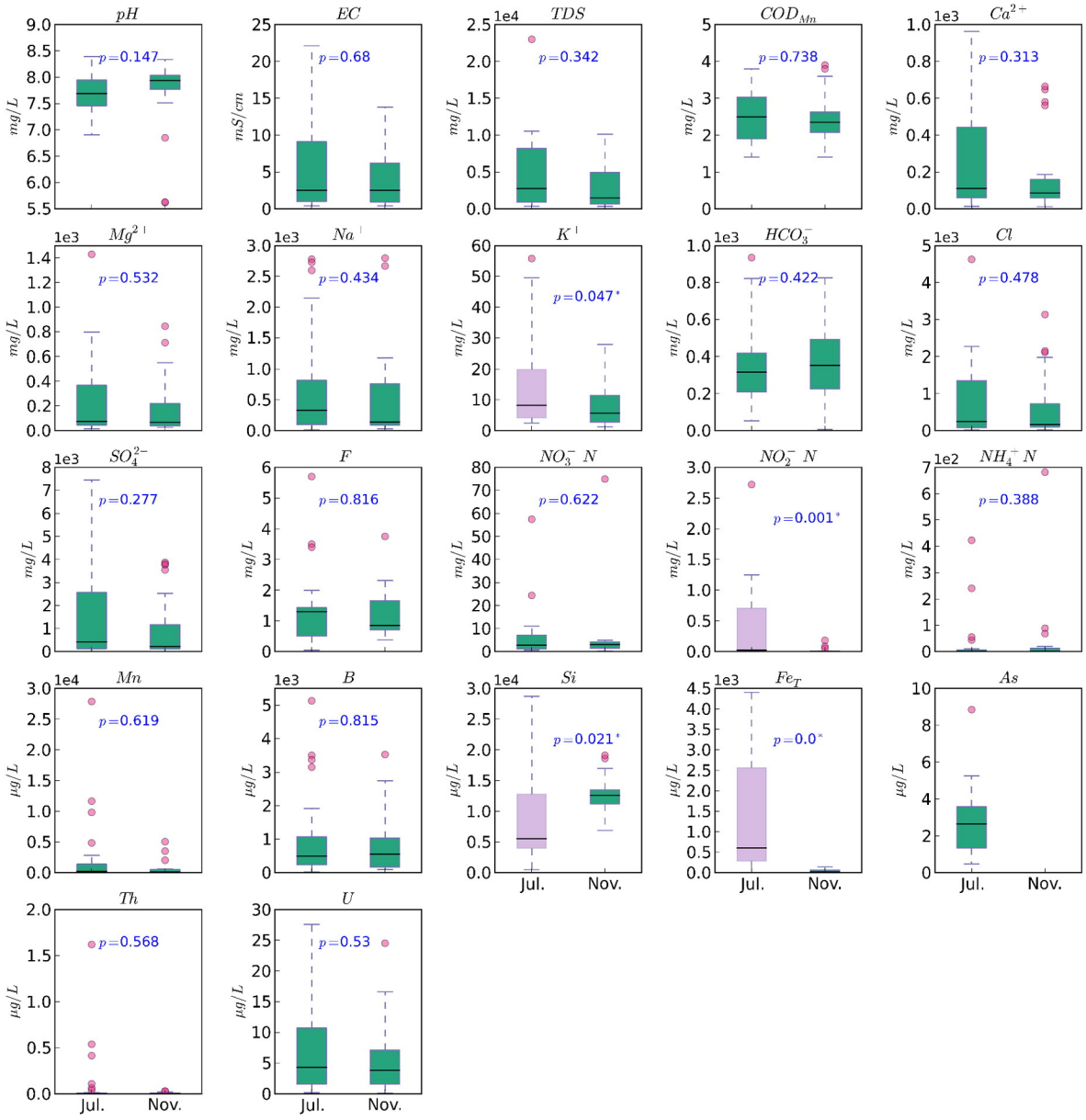

Fig. 3. Boxplot representations of the upper and lower quartiles (box), 2.0× interquartile range (whiskers), median (black line) and outliers (pink circles) for selected variables from all water samples in the wet season (Jul.) and dry season (Nov.) 2013. The outliers are pond-related waters and leachates; see texts in Section 3.1 for detailed information. Different colors of boxes within each panel show significantly different data distributions ($p < 0.05$ with an asterisk) according to the Mann–Whitney U test. (For interpretation of the references to color in this figure legend, the reader is referred to the web version of this article.)

analysis (HCA), analysis of variance (ANOVA) and nonparametric tests were performed using SPSS 22®. Because all the data are generally skewed with the large concentration ranges and outliers (Fig. 3), they were log-transformed after expressed with the same units (mg/L), except for pH and EC (mS/cm). Most log-transformed data (except for the pH) successfully passed the log-normal distribution test based on

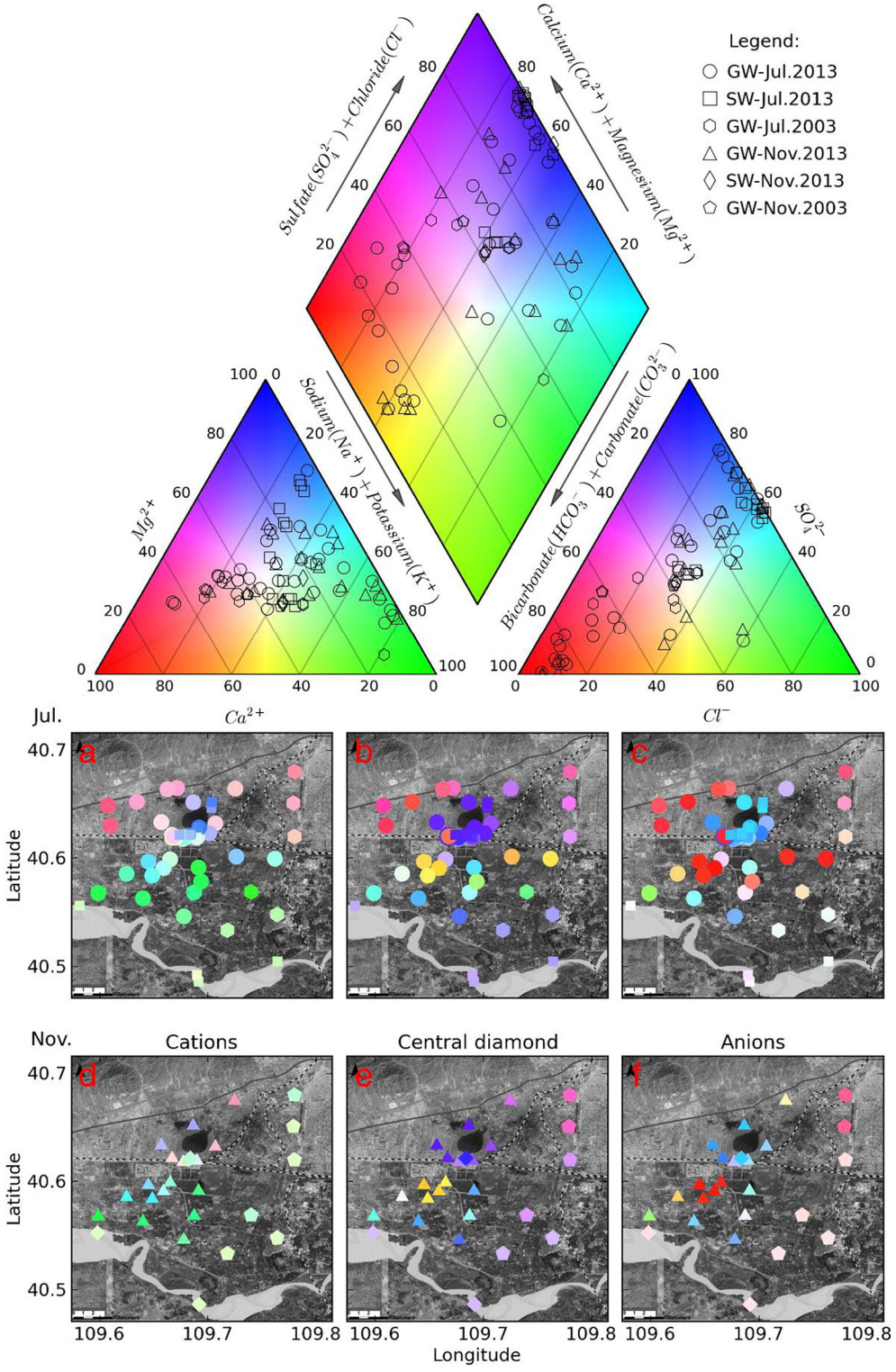

Fig. 4. Color Piper diagrams spatiotemporally visualizing hydrogeochemical facies of water samples from shallow aquifers around the Bayan Obo tailing pond. Sample locations (see Fig. 1.) are color-coded (continuous HSV color scheme) for displaying hydrogeochemical data in space. It can temporally project [i.e., the first row of map (a, b, c) is for Jul. and second row of map (d, e, f) for Nov.] cations (i.e., a and d) and anions (i.e., c and f) onto the map separately. Dot colors represent a proportion of cations or anions as shown on their respective trilinear plots. The color of each dot on the central column map (b and e) corresponds to the central diamond of the Piper plot. For example, green dots on the cation plots (a and d) represent a high proportion of Na^+ and K^+, red dots a high proportion of Ca^{2+} and blue dots a high proportion of Mg^{2+}, while yellow indicates approximately equal proportions of cations. On the anion plots (c and f) green represents high proportion of Cl^-, red a high proportion of ($HCO_3^- + CO_3^{2-}$) and blue a high proportion of SO_4^{2-}, while yellow indicates approximately equal proportions of the anions. (For interpretation of the references to color in this figure legend, the reader is referred to the web version of this article.)

the P–P plots, Q–Q plots and Kolmogorov–Smirnov test. In order to have equal weight in the statistical analysis for each variable, all parameters were standardized by their standard scores (z-scores) (e.g., Ledesma-Ruiz et al., 2015; Biswas et al., 2012). When a concentration was below its detection limit, a value corresponding to 50% of the respective detection limit was used in the statistical analysis.

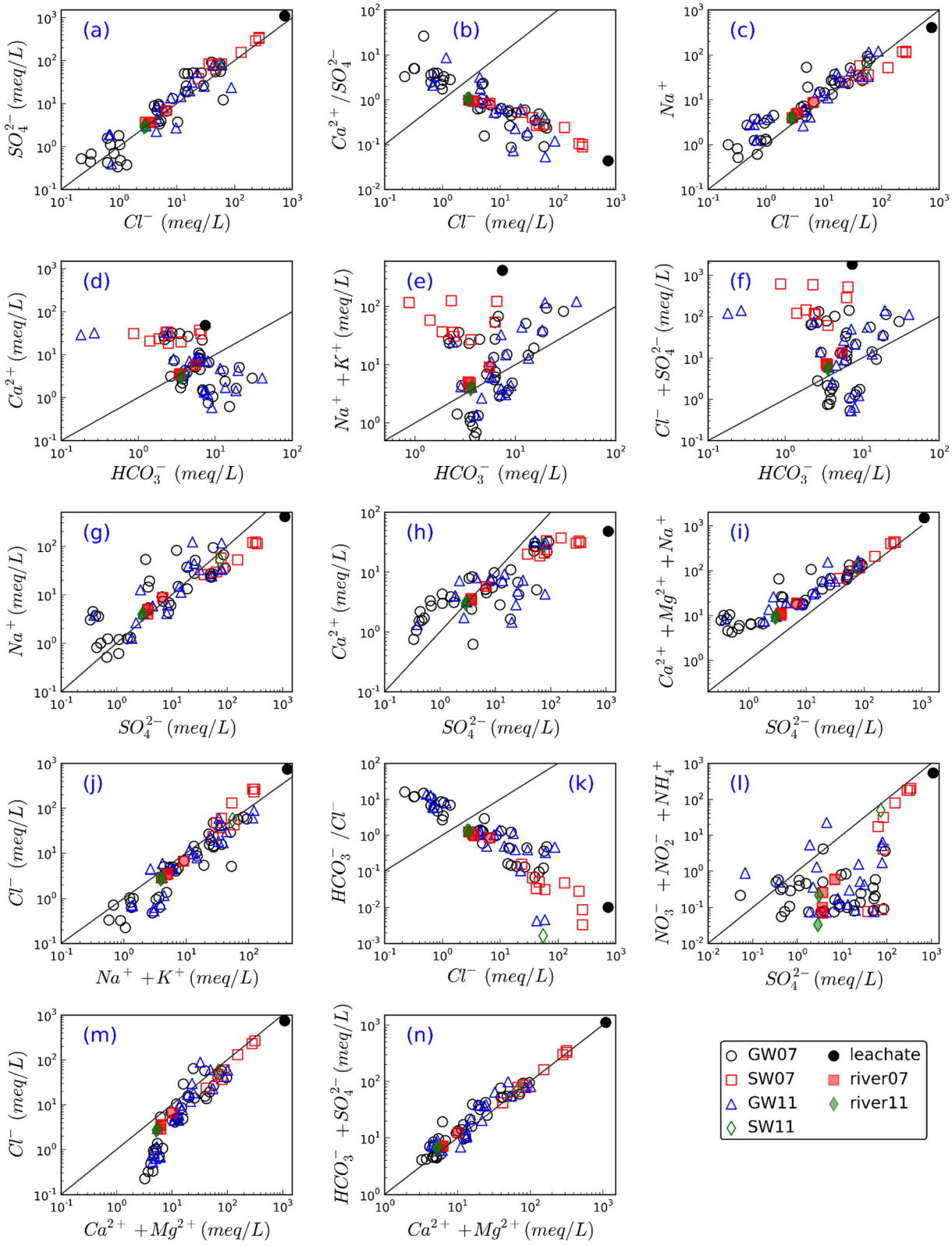

Fig. 5. Ionic ratio evolution and bivariate diagrams showing major relationships to elucidate geochemical reactions. The diagonal solid lines are lines of 1:1 slope. The symbols are kept the same hereafter if there are no special notes.

3. Results

3.1. Leachate and pond-related waters

The leachate sample (pore-water below the tailing-beach) has the highest concentrations among all water samples (Figs. 3, 4, 5, 6 and 7) and can be classified as saline water (TDS > 10,000 mg/L), with EC (113.3 ms/cm), Mg (12,752 mg/L), Na (9371 mg/L), Cl (26,165 mg/L), SO_4^{2-} (52,915 mg/L), NH_4^+ (7,541 mg/L) and Mn (190.710 mg/L). By contrast, concentrations of these elements in the pond-associated water samples [i.e., supernatant water (KL1, KL2, KL3), collection-trench water (SG1, SG2, SG3, SG4) and slurries water (KJ)] exhibit large variations and generally hold second highest values. The swamp waters (i.e., QT6, QT7, QT8), which were collected at the foot of the tailing dam and nearest to the GW06, GW07 and GW08 monitoring wells, also share similar ranges of concentrations with the leachate sample and pond-related waters. The emerged swamp waters were considered as leachates overflowing the land surface (Wang and Tu, 1990). The concentration of uranium (U) and thorium (Th) in leachate sample is 37.8 and 0.064 μg/L, respectively. Briefly, the leachate and pond-related waters display the elevated concentrations of all elements, which occupy outliers in the boxplot (Fig. 3). The dominant anions, Cl^- and SO_4^{2-}, in the pond water show a similar trend to those of Na^+ and Mg^{2+}.

3.2. Yellow river waters

Major ions and other parameters (T, pH, EC and TDS) of six river water samples generally share similar features. They are characterized by moderately alkaline pH (ranging from 7.85 to 8.22 with an average value of 8.09) and low TDS contents (ranging from 568 to 1630 mg/L with average of 997 mg/L). Na^+ and Ca^{2+} dominate cations in these river waters while, the prevailing anion is HCO_3^- (with average of 236.7 mg/L). For trace elements, the concentrations of silicate range from 2393 to 7190 μg/L and those of U from 3.76 to 5.07 μg/L. However, Th concentrations are generally below the detection limit of 0.002 μg/L.

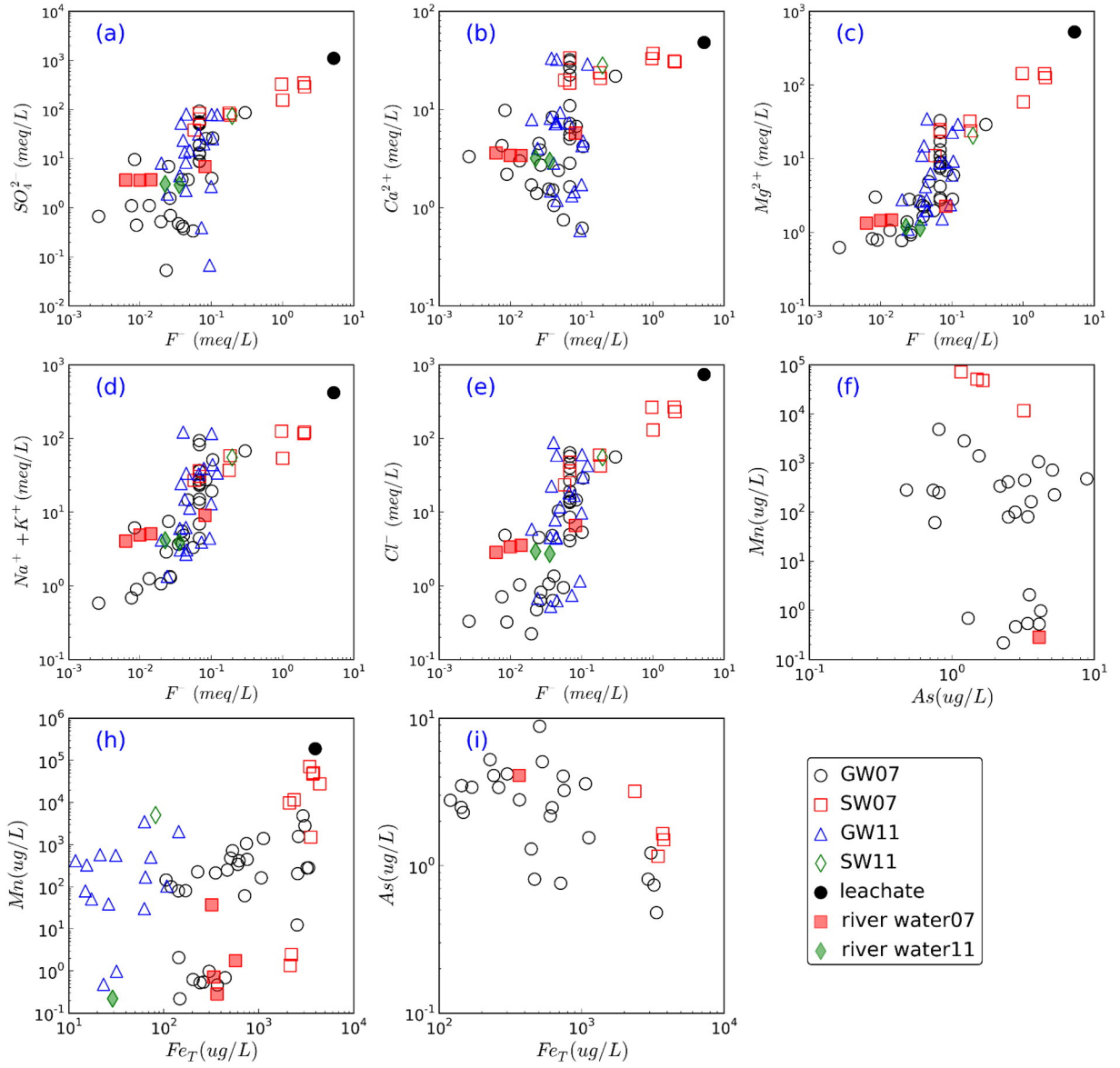

Fig. 6. Scatterplots of relationships between selected variables: (a) SO_4^{2-} vs. F^-; (b) Ca^{2+} vs. F^-; (c) Mg^{2+} vs. F^-; (d) ($Na^+ + K^+$) vs. F^-; (e) Cl^- vs. F^-; (f) Mn vs. As; (h) Mn vs. Fe; (i) As vs. Fe. The symbols are kept the same hereafter if there are no special notes.

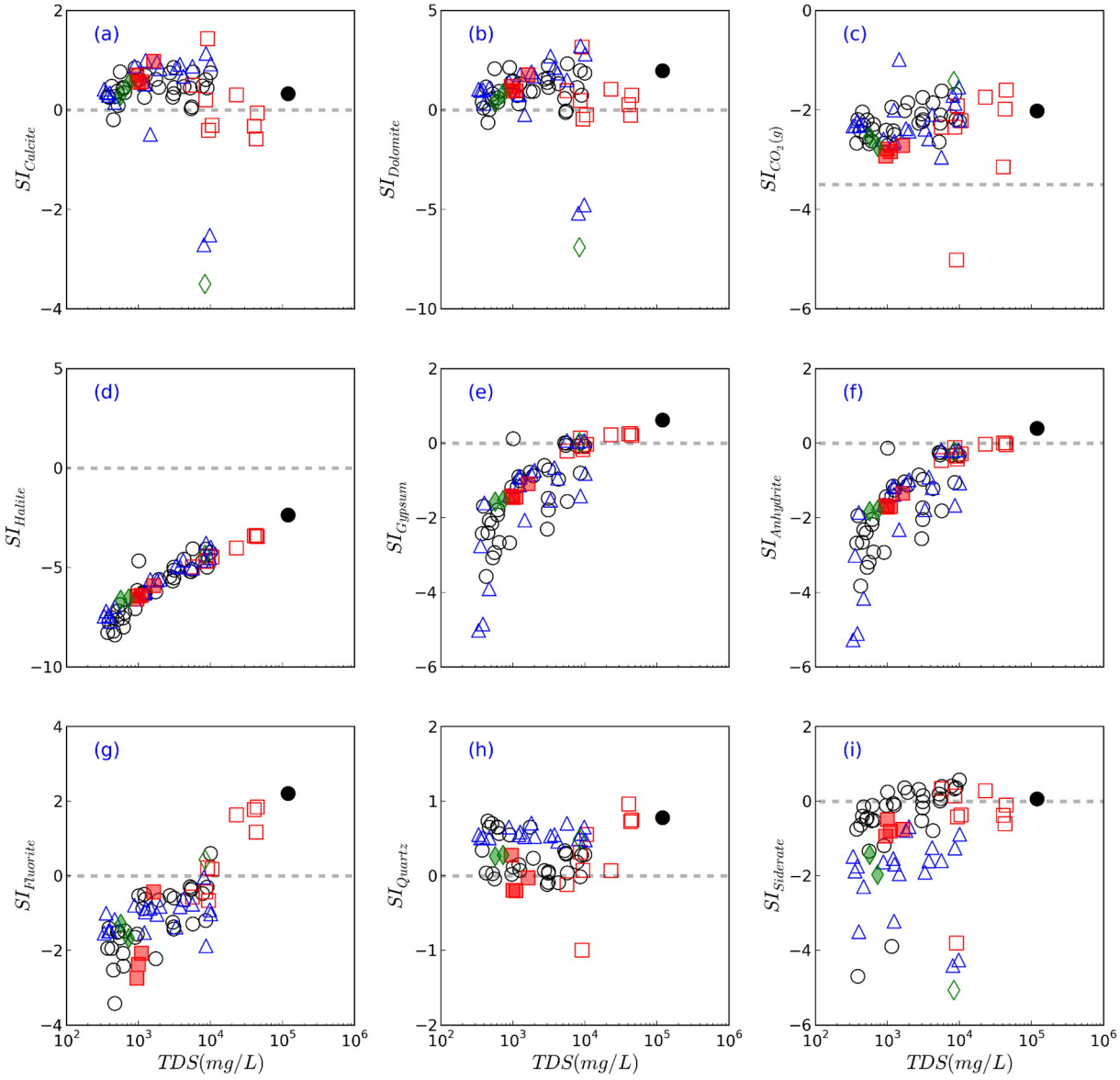

Fig. 7. Saturation indices of water with respect to the selected mineral phases and partial pressure of CO_2. Thermodynamic data are from PHREEQC (Parkhurst and Appelo, 1999).

3.3. Groundwater

The temperature of all groundwater samples varies from 8.6 to 13.1 °C, with an average temperature of 9.8 °C, which is consistent with annual average of air temperature at the Baotou site. The pH ranges between only slightly acidic and moderately alkaline i.e., between 5.6 and 8.4, with a mean of 7.7 for groundwater (compared to 7.5 for surface water). The EC in the groundwater changes considerably from 0.39 to 13.8 mS/cm and the corresponding TDS ranges from 334 to 10,100 mg/L. A large fraction (85%) of the groundwater samples can be classified as brackish due to the high TDS content (1000 mg/L ≤ TDS ≤ 10,000 mg/L). Seasonal differences are evident for certain species between wet and dry sampling periods ($p = 0.05$), in particular for K, NO_2^--N and dissolved Fe and Si (Fig. 3). Generally, Na^+ and Cl^- exhibit large and similar variation in their concentrations; their standard deviations (SD) are larger than their means.

Likewise, Mg^{2+}, SO_4^{2-}, NO_3^--N and NH_4^+-N show a considerable variability with their standard deviation being larger than their mean. According to the National Chinese drinking water (NCDW) guidelines, SO_4^{2-}, Cl^-, F^- and NO_2^--N exceed their critical concentration levels in 56.4%, 47.4%, 54.3% and 35.7% of all water samples, respectively. The F^- concentrations exceed NCDW standard of 1 mg/L in the majority of groundwater samples (78%). The concentrations of SO_4^{2-} and Cl^- are the highest among all dissolved elements in these groundwater samples (ca. 95%). In addition, the high HCO_3^- concentrations occur in groundwater at several locations (e.g., GW16, GW17). In the downgradient areas, about 32% of groundwater samples exhibit an intermediate (mixed) chemical character between Ca^{2+}–Mg^{2+}–Cl^- and Ca^{2+}–Mg^{2+}–SO_4^{2-} hydrogeochemical facies. The Piper diagram modified from Peeters (2014) shown in Fig. 4 indicates that groundwater share a similar composition, predominantly of a Ca^{2+}–Mg^{2+}–Cl^- or Ca^{2+}–Mg^{2+}–SO_4^{2-} type with little difference between the wet and dry periods. Meanwhile groundwater samples are slightly more Na^+–Cl^-– and HCO_3^--rich.

Bivariate comparisons show a number of linear relationships by various bivariate plots (Fig. 5). There are strong positive correlations between Cl^- and SO_4^{2-} ($r^2 = 0.98$, Fig. 5a), Na^+ and Cl^- ($r^2 = 0.89$, Fig. 5c), Na^+ and SO_4^{2-} ($r^2 = 0.85$, Fig. 5g), Cl^- and ($Na^+ + K^+$)

(r^2 = 0.90, Fig. 5j), and ($HCO_3^- + SO_4^{2-}$) and ($Ca^{2+} + Mg^{2+}$) (r^2 = 0.99, Fig. 5n). However, the negative correlations, for example, the Ca^{2+}/SO_4^{2-} molar ratio decrease with increasing Cl^- contents (Fig. 5b) and negative linear trend of HCO_3^-/Cl^- vs. Cl^-, as shown in Fig. 5k. The plot for SO_4^{2-} vs. NO_3^- (Fig. 5l) suggests a lack of a clear relationship. Further, ($Ca^{2+}+Mg^{2+}$) largely contributed to the total cations (TZ^+), while the contribution from ($Na^+ + K^+$) was lower. Concentrations of F^- generally show a good correlation with SO_4^{2-}, Ca^{2+}, Mg^{2+}, and Cl^- (Fig. 6). Fig. 6h displays a positive correlations between Fe and Mn with different trends corresponding to seasonal changes. Despite significant concerns of potential radioactive contamination induced by the Bayan Obo tailing pond, the concentrations of U range from 0.126 to 39.1 μg/L, while lower concentrations of Th (ranging from <0.002 to 0.01 μg/L) are observed in surrounding shallow groundwater. In general, Se, Hg, Pb and Cd are at very low concentrations and below the critical NCDW limits, and thus their behaviors will not be discussed further in this study.

3.4. Speciation–solubility calculations

Speciation–solubility calculations were used to evaluate the geochemical evolution of different water samples and identify the most important controlling geochemical reactions (Appelo and Postma, 2005; Han et al., 2014). Fig. 7a, b, h show that almost all the samples are saturated or oversaturated with respect to calcite, dolomite and quartz, with trends being independent of TDS. On the other hand, halite, gypsum, anhydrite, fluorite and siderite were under-saturated in most of the samples, except for several pond-water-related samples (Fig. 7d, e, f, g, i). These minerals all show remarkable positive trends with increasing TDS (Fig. 7d, e, f). The partial pressure of carbon dioxide (CO_2) varied from $10^{-0.9}$ to $10^{-5.0}$ atm. (Fig. 7c). The relatively lower values (less than $10^{-3.5}$) of CO_2 occur in surface waters with higher TDS.

3.5. Multivariate statistical results

Two principal components were identified to explain 80.04% of the total sample variance (61.59% for PC1 and 18.45% for PC2) for

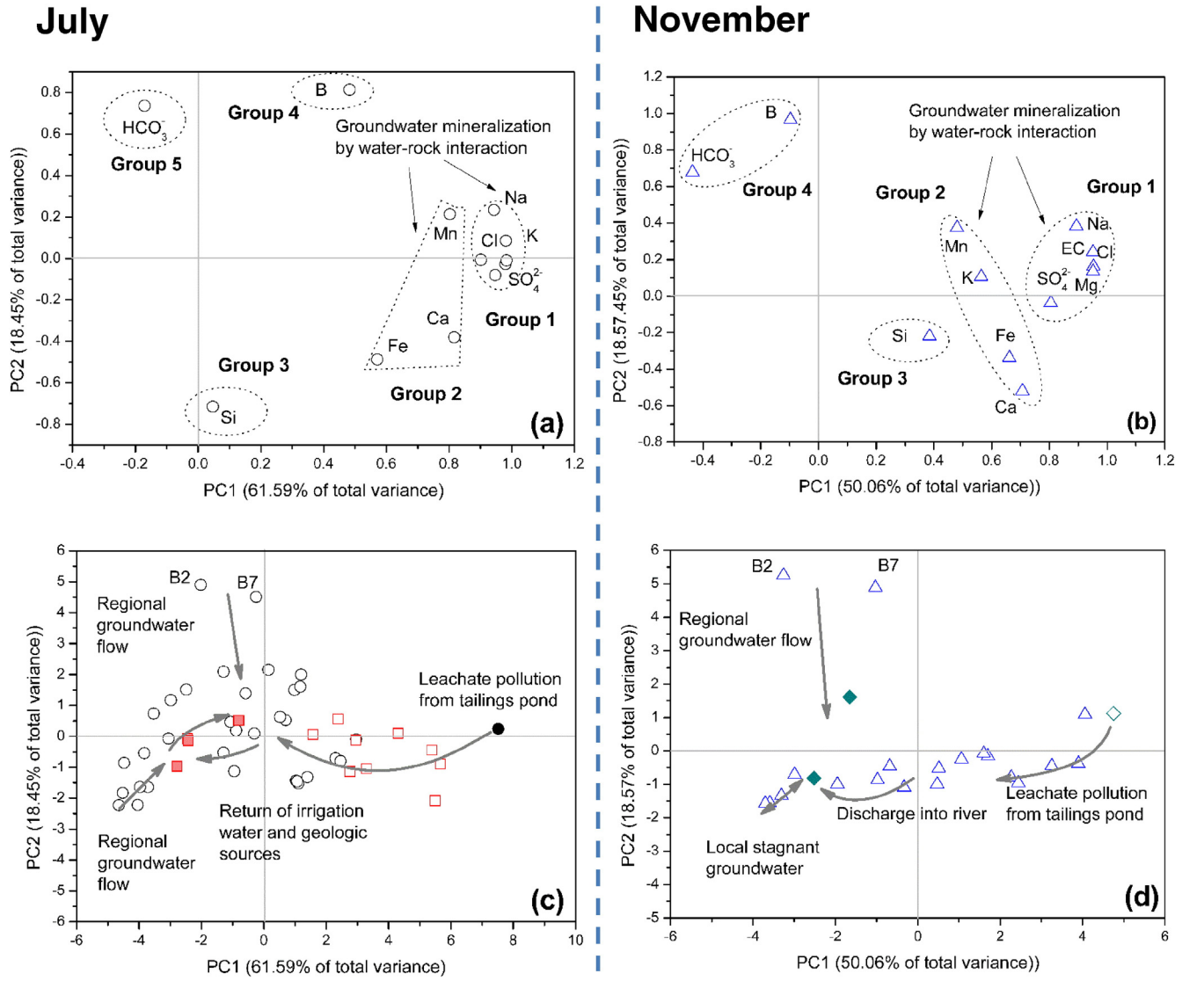

Fig. 8. Results from the PCA for selected chemical components in water bodies surrounding the Bayan Obo tailing pond, showing the plots of variables and loadings; (a) and (b), principal component loadings for water samples in Jul. 2013 and Nov. 2013, respectively; (c) and (d), component scores for water samples in Jul. 2013 and Nov. 2013, respectively. Variables were log-transformed and standardized.

samples collected in July 2013 (Fig. 8a, c), and 68.63% of total sample variance (50.06% for PC1 and 18.57% for PC2) in November 2013 (Fig. 8b, d). In the wet season sampling period, five groups of samples were identified in Fig. 8a. The PC1 factor shows high positive loading for most variables except for the negative loading of HCO_3^-. The results from the HCA in Supporting information Fig. S4 show little differences between summer and winter samples and three main groups were classified.

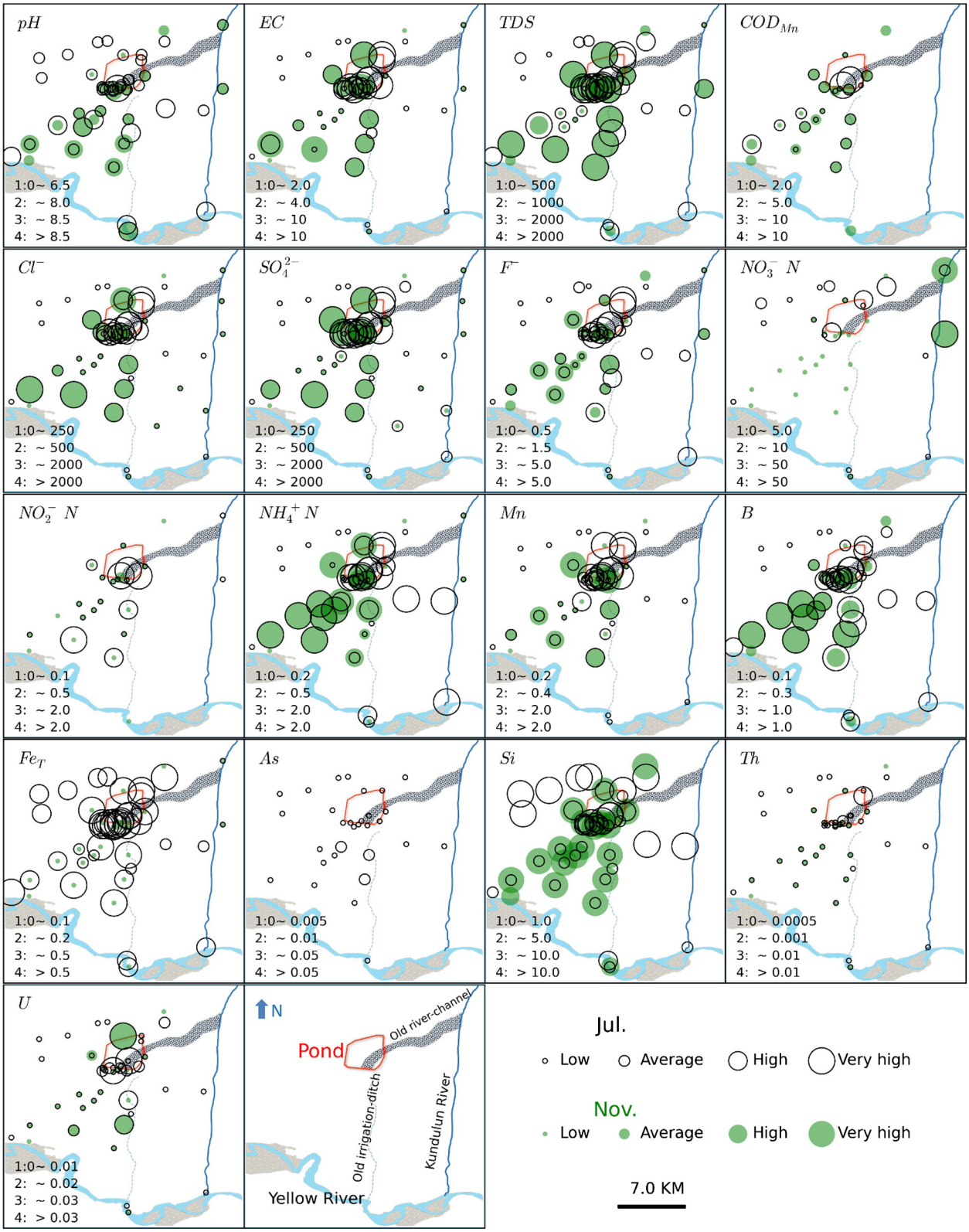

Fig. 9. Spatial distribution of selected pollution indicators (EC, TDS, pH, CODmn, Cl^-, SO_4^{2-}, F^-, NO_3^--N, NO_2^--N, NH_4^+-N, Mn, B, Fe, As, Si, Th, U) from water bodies in the vicinity of the Bayan Obo tailing pond during wet and dry season sampling periods. Values are classified according to the World Health Organization (WHO) drinking water guidelines and National Chinese (NC) groundwater quality standards expressed in (mg/L) except for the pH and EC (mS/cm). All symbols are labeled in the last panel.

4. Discussion

Regional background groundwater is recharged by precipitation in the Wulashan to the north outside the study area. Such groundwater is modified into local groundwater in the study area by mixing with the pond leakage, by precipitation and dissolution, redox and ion-exchange reactions during water–rock interaction, and by other anthropogenic activities. Rainwater with very low concentration for most elements (Guo et al., 2011) can recharge into local groundwater and dilute it in wet season.

4.1. Regional variations, mixing and pond leaking

Our data reveal clear regional variations in hydrogeochemical signatures from the pond towards the downgradient Yellow River, whereby the identified groundwater types varied strongly, as illustrated in Fig. 4. Another observed trend is that the concentration of many species such as Mn, F^-, Fe, SO_4^{2-} decreased with increasing distance from the pond while rebounding to more elevated concentrations closer to the Yellow River (Fig. 9). Since the tailing pond has been operated for over 50 years without strict documented protections, many previous reports expressed serious concerns that a severe contamination plume must have evolved and extended downstream all the way towards the shallow aquifer regions of the Hubao plain (e.g., Fang, 2006; Guo and Tong, 2011; Pan, 2010; Huang et al., 2014). However, the data collected to date suggest unconnected plumes along the main flow paths (e.g., for SO_4^{2-}), as shown in Figs. 4 and 9. Besides significant mixing processes (Figs. 5a, b, c, k and 6c, d, e) between tailing pond leakage as well as irrigation water with the ambient groundwater, several other anthropogenic and geogenic factors appear to contribute to the evolution of the groundwater hydrochemistry in the study area.

Although the Bayan Obo ore has a high abundance of Fe-bearing minerals (e.g., magnetite, hematite) and is well known for enriched REEs, only iron was extracted in earlier decades. Some sulfide gangue minerals (e.g., pyrrhotite, sphalerite and pyrite) were also detected in tiny amount in the tailings. That suggests that there might have been a substantial accumulation of products from oxidation of sulfide in the tailings and therefore there should be a high risk for AMD generation. However, contrary to those expectations there is no acid water discovered, while high concentrations of SO_4^{2-} and total dissolved iron do indeed persist (see Figs. 3 and 9) (Fang, 2006). This can be attributed to the substantial buffering capacity that is provided by the prevailing carbonates (dolomite and calcite). The consumption of those minerals can explain the high concentrations of Mg^{2+} and Ca^{2+}, together with the relatively low HCO_3^- concentrations. Fig. 9 also displays the occurrence of NO_3^--N and NO_2^--N, which partially originates from pond leakage but also from fertilizers. Interestingly, the concentration of boron increases as groundwater moves away from the pond, indicating that there were still other anthropogenic pollutants such as the application of agricultural chemicals (pesticides). Briefly, high Cl^-, SO_4^{2-}, Na^+, NH_4^+-N, B and U contents among the examined well water samples collected from in or near residences (GW12, GW15, GW14, GW16, GW17, GW18) may have originated from household sewage and industrial waste water, less homogeneous sediments, and other anthropogenic activities such as fertilizer, manure, and animal water applications. In order to precisely estimate the sources of ammonia, boron and sulfate, however, their isotopes should be analyzed in future.

It should be noted that, higher concentrations of TDS, EC, SO_4^{2-} and Cl^- were found in shallow wells rather than in deep wells, which were most likely attributed to serious salinization in soil and shallow groundwater caused by high evapotranspiration in arid regions (e.g., Bauer et al., 2007), if neglecting other anthropogenic contributions and/or local point contamination sources. This is also consistent with their seasonal changes in concentrations in Fig. 9. Because of the differences of precipitation strength between wet and dry periods the fluctuations of water table could have effects on redox conditions in the upper layer of aquifer. This means that the observed seasonal changes of some species (e.g. Mn and Fe) is probably caused by combined effects from higher concentrations in the upper layer induced mainly by strong evapotranspiration and sampling depth below the water table.

Here, it could reasonably be inferred that in the absence of impervious liners the leakage into the shallow aquifer might have been highest in the early phase of the pond operation while fine-grained materials, slimes and increasing compaction must have resulted in decreasing hydraulic conductivities and decreasing leakage rates in the later phase of the pond operation. The regional groundwater flow further diluted and attenuated elevated concentrations of contaminants in downgradient direction of the tailing pond. Southern areas containing many lenses of silty clays adjacent to the Yellow River are generally considered as natural flow barriers, consequently decreasing the transport rates and leading to an appreciable amount of contaminant stagnation within this relatively stagnant flow zone. As shown in Fig. 9, the channel of an old irrigation ditch might also provide a preferential flow path for solutes and enhanced contaminant mass fluxes may occur towards this area. This is consistent with the higher concentrations in GW14, GW16 and GW18 compared to other nearby monitoring wells.

In summary, many groundwater samples directly carry the signature of pond leakage but there are also samples with more complex mixed signature (see Figs. 4, 5, 6, 7, and 9). The reasons for the latter are probably that the pond leakage signature is affected by additional (i) water–rock reactions that occur along the flow path and (ii) other local anthropogenic impacts, such as irrigation activities along with fertilizer utilization, nearby factories and/or domestic drainages into groundwater.

4.2. Precipitation and dissolution

We observed a clear Ca^{2+}/SO_4^{2-} molar ratio decreasing with an increase in Cl^- contents (Fig. 5b), which indicates that gypsum acted as a sulfate source (Merchán et al., 2015). The positive constant Na^+/Cl^- ratio (Fig. 5c) and good correlation between ($Mg^{2+} + Ca^{2+} + Na^+$) and SO_4^{2-} (Fig. 5i) demonstrated dissolution of halite and gypsum. Similar to Ca^{2+}/SO_4^{2-} vs. SO_4^{2-}, a negative linear trend of HCO_3^-/Cl^- vs. Cl^- is shown in Fig. 5k, and approximately 69.5% of samples showed HCO_3^-/Cl^- ratios lower than 1.0, which means the water bodies were significantly affected by salinization (Monjerezi et al., 2011), which is in accordance with previous geochemical studies (e.g., Fang, 2006; Si et al., 2015). There were negative relationships between Ca^{2+}, Mg^{2+} with HCO_3^- (Fig. 5d, Fig. S5), suggesting that their concentrations were controlled in a large part by solubility product of carbonates above saturation. However, a majority of samples reflect an extra source of these cations compared to only dissolution of carbonate because of no significant relationships in Fig 5e. These extra cations were balanced by Cl^-, SO_4^{2-} (Fig. 5f) and/or silicate weathering (congruent and incongruent silicate dissolution) (e.g., Lghoul et al., 2014), but with limited contribution from carbonate dissolution. The high concentrations of Na^+ and SO_4^{2-} have a good positive correlation (Fig. 5g), which might be caused by the dissolution of sodium sulfate minerals, as revealed in earlier documents (e.g., Zhu, 1962; Zheng, 1992). If Ca^{2+} and SO_4^{2-} contents are mainly controlled by gypsum and anhydrite, then their ratio is near 1.0. Fig. 5h shows that Ca^{2+} exceeds the 1:1 line at lower SO_4^{2-} content and vice versa. Examination of Fig. 5h, i, n and d suggested that dissolution of calcite, dolomite, and gypsum exerted a significant control on Ca^{2+}, Mg^{2+}, SO_4^{2-}, and HCO_3^- contents. A poor relationship of SO_4^{2-} with nitrogen (Fig. 5l) might suggest that the high SO_4^{2-} concentrations are not related to agricultural activities, but there might exist denitrification of nitrate and reduction of sulfate. In comparison to the contributions from pond leakage and geogenic sources, the amount of sulfate derived from agricultural activities appears to be negligible. The excess of Na^+ over K^+ (Fig. 5c, j) is presumably related to the slower weathering rates of potassium-bearing minerals. The dominance of Na^+ mainly resulted from mixing of the pond leakage and local groundwater, and secondly from silicate and halite weathering and/or dissolution. Unlike the

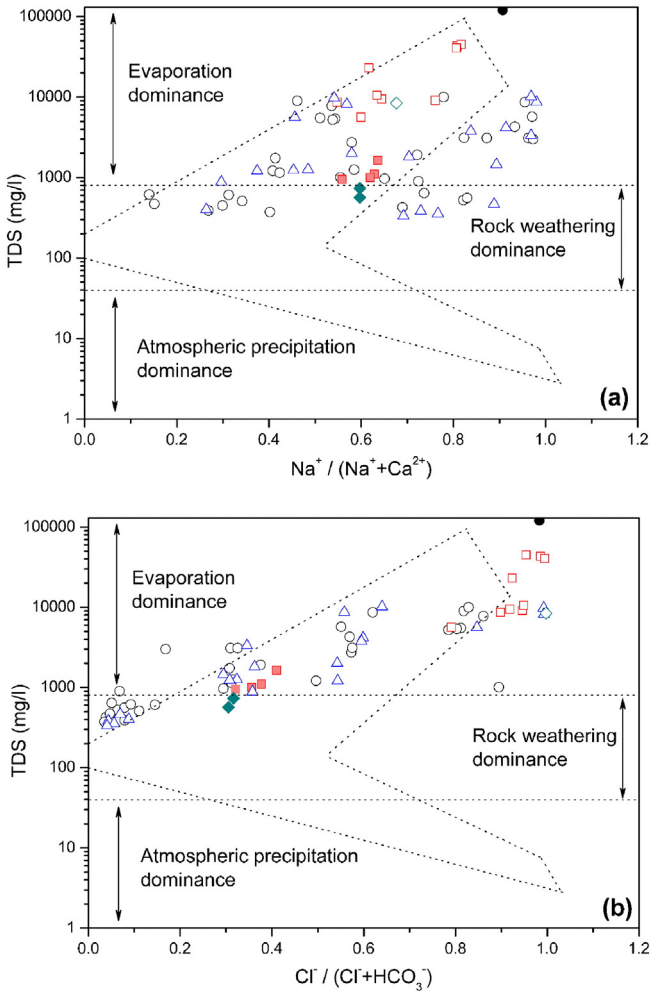

Fig. 10. Gibbs plots of (a) TDS vs. $Na^+/(Na^+ + Ca^{2+})$ and (b) TDS vs. $Cl^-/(Cl^- + HCO_3^-)$, reflecting generally dominant processes that control the groundwater chemistry in the study area.

results of Monjerezi et al. (2011) and Ledesma-Ruiz et al. (2015), we observed that Ca^{2+} and Mg^{2+} were the primary cations in any mineralization conditions. Apart from mineral dissolution and precipitation, the increase of $(Ca^{2+} + Mg^{2+})$ with increasing Cl^- concentrations (Fig. 5m) may be in part due to reverse ion exchange in the clay/weathered layer (e.g., Jankowski et al., 1998).

Fig. 10 displays Gibbs diagrams of TDS concentrations against the weight ratios of $Na^+/(Na^+ + Ca^{2+})$ for cations and of $Cl^-/(Cl^- + HCO_3^-)$ for anions (e.g., Xie et al., 2015). It shows that all samples fall into the evaporation and weathering zones, indicating the potential of evaporation and/or the dissolution of evaporites during weathering in the studied area. Accumulations of evaporites, such as halite (NaCl), anhydrite ($CaSO_4$) and gypsum ($CaSO_4 \cdot 2H_2O$), in topsoil and farmland were previously reported in Zheng (1992) and Wang (2006). Wind-driven, muscovite-bearing dusts originating from tailings were also extensively distributed across the land surface. As supported by Figs. 5c, i and 7d, e, f, dissolution of evaporites via infiltration and subsequent transport mixing of leachate with shallow groundwater, can significantly increase the concentrations of Mg^{2+}, Ca^{2+}, Na^+ and SO_4^{2-} in groundwater. As shown in Fig. 10, a few samples which were mostly collected from the piedmont and flow-through areas, i.e., the northern part of the pond and its vicinity, controlled by rock weathering, reflecting the significance of water–rock interactions. On average, $(Na^+ + K^+)$ are together contributing 31% of the total cations (TZ^+), $(Ca^{2+} + Mg^{2+})$ contributing 46% of the TZ^+, relatively high $(Ca^{2+} + Mg^{2+})/HCO_3^-$ (0.8–150.1) and relatively low $(Ca^{2+} + Mg^{2+})/(Na^+ + k^+)$ (0.41–3.1) (Supporting information Fig. S5) ratios suggest that carbonate dissolution is relatively dominant than silicate weathering (e.g., Monjerezi et al., 2011; Singh et al., 2012).

4.3. Redox processes

High concentrations of dissolved Mn and Fe are frequently associated with reducing conditions and their concentration levels are mainly controlled by the pH and Eh of the waters (e.g., Buschmann et al., 2007; Han et al., 2014). In this study, similar to Buschmann et al. (2007), a weak but positive correlation was observed between Mn and Eh (see Supporting information Fig. S6). Typically, lower pH will enhance the dissolution rates of both iron and manganese oxide and hydroxide. Additionally, Fe and Mn concentrations show positive correlations with SO_4^{2-}, Cl^- and TDS (see Supporting information Fig. S6), which is consistent with the oxidation of remnant sulfide-bearing minerals, perhaps accompanied by anaerobic microbial processes that might also contribute to high the concentrations of Fe and Mn. High Mn concentrations were observed in combination with a wide range of Fe concentrations, but mainly in conjunction with high Fe concentrations. Considering that Mn has a strong affinity for Fe oxides, the co-precipitation with Fe oxides may remove dissolved Mn via sorption onto precipitated Fe hydroxide (Appelo and Postma, 2005). However, the relationship between Fe and Mn is not simply linearly relevant in Fig. 6h, but their positive relations represent seasonal changes of redox conditions (see Figs. 3, 9). Under this condition, the reductive dissolution of Fe oxide/hydroxide is the dominant geochemical process and results in the mobilization of As in groundwater. This inference can be confirmed by the observed inverse correlation between total dissolved As and Fe in groundwater collected in July, the wet and irrigation period. Additionally, slightly elevated As concentrations (up to 8.85 μg/L) were observed in SO_4^{2-} poor (not show here) and slightly Fe-rich (Fig. 6i) environments, similar to the trends reported by Han et al. (2014) and Xie et al. (2015). This suggests that the Fe(III)-SO_4^{2-} redox cycling induced by irrigation practices in this area may contribute to the presence of As in groundwater.

4.4. Ion exchange processes

Cation exchange might be another factor contributing to high concentrations of Mg and Ca. As Jankowski et al. (1998) and Xie et al. (2015) noted, if ion exchange was the dominant process in the system, the relationship between $(Na^+ - Cl^-)$ and $(Ca^{2+} + Mg^{2+} - SO_4^{2-} - HCO_3^-)$ should be linear with a slope of −1. Fig. 11a depicts a goodness of linear fit ($n = 66$, $r^2 = 0.85$, $p < 0.01$) with a slope of −0.78 for a majority of groundwater samples, clearly pointing to the existence of Na ion exchange for Ca and Mg. The pond- and leachate-related water samples shift away from the linear regression line, demonstrating they are derived from different source. Furthermore, a majority of samples having negative CAI1 (i.e., $[Cl^-(Na^+ + k^+)]/Cl^-$) and CAI2 (i.e., $[Cl^-(Na^+ + k^+)]/(SO_4^{2-} + HCO_3^- + CO_3^{2-} + NO_3^-)$ indices in Fig. S7 (in Supporting information) also provides additional supporting evidence of reverse ion exchange (e.g., Biswas et al., 2012). In order to discriminate which ion (Ca, Mg or Ca + Mg) dominantly controls such hydrogeochemical reaction, their relationships with (Na–Cl) were developed in Fig. 11b, where the slope and correlation coefficients between the X and Y-axes suggest that the significant correlation ($n = 7$, $r^2 = 0.71$, $p < 0.05$) is for the exchange of Na for Ca, indicating that equivalent portions of Ca are exchanged for Na.

4.5. Source of fluoride

The origin of the high level of F^- in the groundwater surrounding the tailing pond needs to be carefully examined because it has been argued that natural geochemical anomalies could be the cause of the elevated concentrations rather than pond leakage. Indeed, high F^- concentrations ranging from 0.5 to 2.0 mg/L in groundwater associated

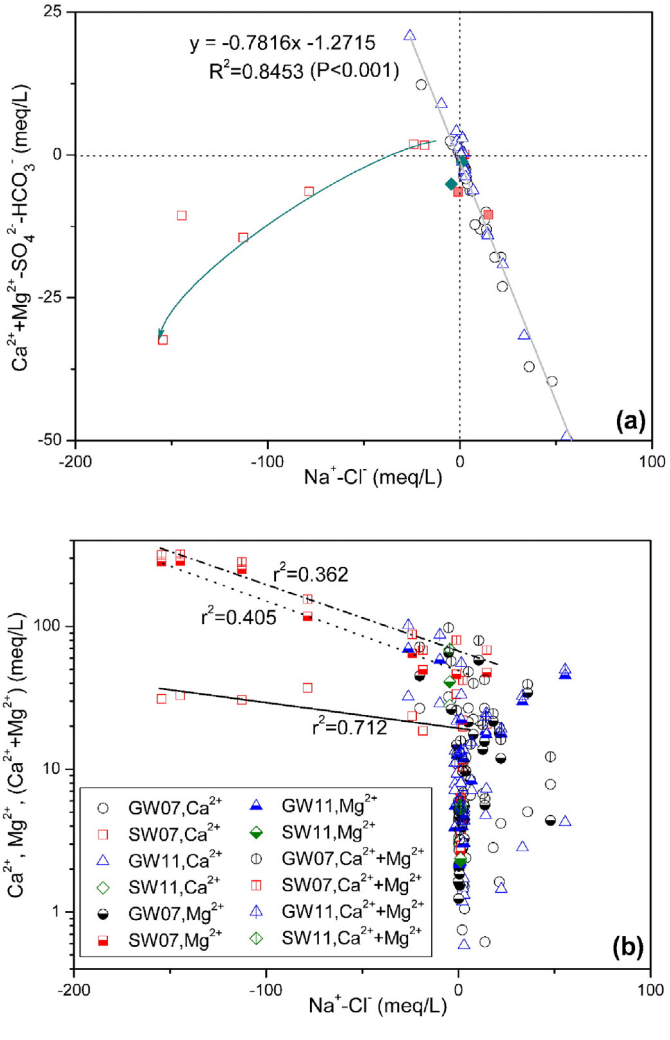

Fig. 11. (a) Relationships between $(Ca^{2+} + Mg^{2+}–SO_4^{2-}–HCO_3^-)$ vs. $(Na^+–Cl^-)$, and (b) Ca^{2+}, Mg^{2+}, $(Ca^{2+} + Mg^{2+})$ vs. $(Na^{2+}–Cl^+)$. All values are expressed in meq/L.

with geogenic sources have already been reported before the construction of the Bayan Obo tailing pond (e.g., Wang and Tu, 1990; Zheng, 1992). Many hydrogeochemical investigations documented that F-bearing minerals (e.g., fluorite) commonly occur in both the Wulashan Mountains and the Yellow River alluvial plain (e.g., Zhu, 1962). Although the leachate and the pond water have higher F^- concentrations, with averages of 40 and 10 mg/L, respectively, the mixing effect in surrounding groundwater seems not to be significant because of low F^- in all groundwater samples. Specially, fine-grained fluviolacustrine sediments and the local stagnant groundwater flow were more likely responsible for the fluoride enrichment. As Zheng and Lu (1986) suggested, the naturally high abundance of soluble fluorite combined with anthropogenic inputs from leakage mixing, infiltration of atmospheric dust and irrigation return flow all contributed to the high-fluoride groundwater in this area. Long-term exposure to high-fluoride groundwater and respiration of F^- borne aerosols were found to be the main reasons for the endemic fluorosis in this region (Zheng, 1992). The bivariate plots in Fig. 6a and e (i.e., SO_4^{2-} vs F^-, Cl^- vs F^-) and Fig. 5a, b, c, g, k all show good linear relationships, indicating that significant mixing occurs along the flow path.

Carpenter (1969) found that in ocean carbonates, i.e. calcite and aragonite, carry more fluoride than apatite does. In this study area the dominant carbonate is dolomite, which has a crystal structure similar to that of aragonite. Therefore, it is reasonably inferred that dolomite is enriched in fluoride as well as in aragonite. In Fig. 6b there is a poor correlation between F^- and Ca^{2+} indicating dissolution of fluorite, apatite and carbonate minerals might not be one of the contributions of fluoride to water. Contrary to F^- vs. Ca^{2+}, F^- contents increased with Mg^{2+} concentrations (Fig. 6c), suggesting that the solubility of biotite and dolomite mainly controlled surrounding groundwater compositions. However, it is possible that that all these F^- containing provided some fluoride to groundwater by dissolution during water–rock interaction. The poor correlation of Ca^{2+} and fluoride is due to disturbance by strong ion exchange of Ca^{2+} with Na^+ (Fig. 11) after dissolution of F^- containing minerals. Relatively weak ion exchange of Mg^{2+} with Na^+ did not substantially change the correlation between Mg^{2+} and fluoride. Additionally, OH^- can replace the exchangeable F^- from F-bearing minerals (F-bearing apatite) because they have similar ionic radii and the same negative charge (e.g., Stumm and Morgan, 1995; Li et al., 2015). Therefore, basic conditions in the current study area can increase dissolved fluoride contents. Fig. 6d shows a pronounced correlation between the abundant contents of $(Na^+ + K^+)$ and F^-, which might be induced by hydrolysis reactions of muscovite and/or biotite (e.g., He et al., 2013). A significant correlation between Cl^- and F^- in Fig. 6e indicates they are originated from the same pollution source. So does SO_4^{2-} and F^- in Fig. 6a. Moreover, we also observed a poor correlation among F^- with NO_3^--N, NO_2^--N, NH_4^+-N and B, suggesting that fertilizer application is negligible for fluoride pollution in this area. This observation agreed well with our PCA and HCA analysis (see above Section 3.5), indicating that F^- is associated with mineral weathering and water–rock interactions.

4.6. Agricultural activities

Elevated concentrations of NH_4^+-N in the downstream areas of the study site (e.g., GW14, GW18) could, in principle, suggest that pond leachate has migrated through a groundwater pathway from the tailing pond into these regions. However, a more plausible explanation of those elevated concentration is that they originate from contamination by the use of waste water from the mining plant for irrigation purposes over several years, as documented for example in Zhu (1962). Pond water use for irrigation (e.g., Thukral, 1989), followed by spatially and temporally variable influences of dilution and evapoconcentration within this relatively slow-flowing or stagnant aquifer zone, indicates that this pollution pathway appears more likely than NH_4^+-N migration within the groundwater. More investigation is needed to resolve this question by analysis of nitrogen isotope compositions in waters in future.

In addition to the use of pond water for irrigation, other types of anthropogenic pollution such as the application of agricultural chemicals (pesticides) have occurred in various areas. Briefly, high Cl^-, SO_4^{2-}, Na^+, NH_4^+-N, B and U contents among the examined well water samples collected from in or near residences (GW12, GW15, GW14, GW16, GW17, GW18) may have originated from household sewage and industrial waste water, less homogeneous sediments, and other anthropogenic activities such as fertilizer, manure, and animal water applications.

4.7. Multivariate statistical discussion

In Fig. 8a, Group 1 and Group 2 could be described by complex mineralization from water–rock interaction and Fe–Mn redox reactions. The Group 3 members (i.e., Si) having low positive loadings for PC1 but high negative loadings for PC2 may be induced by the silicate weathering processes (e.g., albite, K-feldspar, anorthite) and leakage of the tailing pond and/or agricultural fertilizers. The HCO_3^- (Group 5) and B (Group 4) occupying high positive loadings for PC2 but different PC1 values, could be related to extra contributions such as leakage of the tailing pond and/or agricultural fertilizers. Concentrations of B increased with distances away from the pond, such as low fractions of pond-related waters, indicated that Group 4 may be more likely to be caused by other contamination sources that occur in the studied area. By contrast,

Group 5 was very likely related to pond leakage impact because of characteristic high HCO_3^- concentrations of pond-related waters.

Compared with the hydrogeochemical characteristics found for the summer period samples, silicate weathering processes played a less important role in winter, and an increase in loadings related to Fe and Mn, which were due to more reduced conditions in winter. Group 4 is associated with B and HCO_3^- and could indicate a decrease in the calcite weathering process, which may follow boron contamination. The increases in Ca^{2+} and SO_4^{2-} loadings are likely related to the dissolution of evaporitic rocks (e.g., gypsum) and/or cation exchange in winter.

Based on the factor analysis in Fig. 8a, b, we calculated factor scores corresponding to different sampling locations along with possible controlling processes in Fig. 8c, d. The leachate- and pond-associated surface water showed high positive PC1 scores while piedmont groundwater (e.g., B2 and B7) had high positive PC2 scores, indicating that the mixing processes of these two sources of water dominantly contributed to downgradient water quality. In the wet season, the downgradient shallow aquifer was recharged by river water, and then, large areas of irrigation returned flow into the river. Conversely, in the dry season, downgradient groundwater discharged directly into river water, and high evaporation strengthened local stagnant groundwater flow surrounding the pond site. According to the HCA results (see Supporting information Fig. S4), three main groups at the phenon line were classified: the first group (Na^+, Cl^-, Mg^{2+}, SO_4^{2-}, Ca^{2+}) reveals dissolution of gypsum and/or anhydrite; the second (Si, B, HCO_3^-) indicates silicate weathering and additional boron contamination; and the third (Mn, Fe) suggests footprints of redox environment variation and contributions of specific minerals. There is a little difference between summer and winter samples.

Given all that, there is no single significant geochemical mechanism can accurately interpret current chemical composition of the groundwater in the surroundings of the Bayan Obo tailing pond. Admittedly, in this region there exist a high natural geochemical background for As and F (e.g., Smedley et al., 2003) which would conflate their concentrations in groundwater. However, our observed pond leaking and mixing processes, mineral precipitation and dissolution together with redox reactions cannot be ignored. Additionally, regional hydrologic systems with serious salinization in the downgradient alluvial plains (the River-fed aquifers) cannot be understood well without systematically studying occurred salinity transport and the feedback mechanisms among geochemical processes (e.g., Bauer et al., 2007). Thus, the combining effects of these geochemical processes together with physical and geochemical heterogeneities contributed current observed plumes.

5. Conclusions and implications

This study integrated hydrogeochemical characterization and multivariate statistical analysis to examine the groundwater quality of the shallow aquifer downstream of the Bayan Obo tailing pond and to refine understanding of the associated hydrogeochemical evolution. This involved a comprehensive analysis of the physical and chemical processes affecting tailing pond and answering the question whether leakage has been transported through the groundwater system towards the downgradient alluvial plains and discharged into the Yellow River. The main findings and conclusions can be drawn as following:

1) Along the general groundwater flow direction from the tailing pond to the Yellow River, the plumes of inorganic contaminants (Mn, NH_4^+, F^- and SO_4^{2-}) were very likely caused by the pond leakage, with changing hydrogeochemical types and decreasing concentrations progressively further away from the pond. On the other hand, the contamination of NO_2^- is only limited to the area nearby the tailing pond.
2) There might be potential anthropogenic contributions to high levels of boron and silicate with seasonal variability while a large body of dissolved Mn and Fe indicated that reducing conditions were prevalent in the studied area.
3) There is no geochemical evidence for U and Th contamination in groundwater due to leakage from the tailing pond.
4) Combining effects including regional geogenic variations, pond leaking and downstream mixing, mineral precipitation and dissolution, redox processes, ion exchange processes and agricultural activities controlled groundwater hydrogeochemical signatures.
5) Other processes should be considered in coming studies, such as (i) heterogeneous flow regimes induced by regionally/locally small hydraulic gradients and conductivities and potential preferential flow paths from paleo-stream and ditch channels and (ii) density driven effects caused by strong evaporation and shallow depth of water table (e.g., Bauer et al., 2007).

Our study substantiates the negative impacts of the Bayan Obo tailing pond on surrounding shallow groundwater. High hydraulic gradients resulted in relatively high rates of leakage into regional groundwater flow systems, which thus pose adverse impacts on adjacent agricultural activities, the downstream Yellow River, and groundwater-dependent ecosystems. Although the geochemical interpretations presented above is in agreement with the main hydrogeochemical features of the zone of contamination in the aquifer, many detailed characteristics of the plume behavior and associated reactions have not yet been fully defined. Given a complex interplay between chemical, hydrological and physical conditions occurring in the subsurface of the study area, future's stable isotopes tracing (e.g., δD, $\delta^{18}O$, $\delta^{34}S$, $\delta^{15}N$, $\delta^{13}C$, $^{87}Sr/^{86}Sr$, $^{234}U/^{238}U$) together with reactive transport modeling will quantitatively characterize behaviors of contaminants migration. In any case, because the Bayan Obo tailing pond is still active and storing a large volume of slurries containing radionuclides and rare earth elements, further efforts should be made to contain and safeguard the tailing pond area to minimize the risks of widespread contamination to public health and to sustainable economic development in the region. In addition, the joint use of hydrogeochemical interpretation based on knowledge of the hydrogeological setting and multivariate statistical techniques based on multivariate probability distributions can provide a unifying tool to understand major water–rock interactions and supply a scientific basis for protection and rational utilization of groundwater resources in similar tailing-impacted areas worldwide.

Acknowledgments

The authors acknowledge financial support provided by the Ministry of Environmental Protection of China (Grant No. 201309005), the National High Technology Research and Development Program of China ("863" Program) (Grant No. 2012AA062603), the Research Fund of Shaanxi Key Laboratory of Comprehensive Utilization of Tailings Resources (Shangluo University) (Grant No. 2014SKY-WK006), and the National Natural Science Foundation of China (Grant No. 41330632), and Xiang Huang is also supported by a grant from the China Scholarship Council. We are very grateful to Drs. Henning Prommer, Yan Zheng and Grant B. Douglas for helpful discussions and English editing on earlier version of manuscript. We thank Chunli Zheng, Jingchun Yan, Wenjie Ren, Weiguo Gao, Mingang Dong, Xinli An, Haochen Cheng and Juan Liu for their helps of field work. We also appreciate valuable suggestions from the editor and three anonymous reviewers for improving the manuscript.

Appendix A. Supplementary data

Supplementary data (supporting information) file to this article includes original geochemical data in Table S1, background information about the study area in Figures S1 and S2, additional results of water samples in Figures S3 to S8, which can be found online at http://dx.doi.org/10.1016/j.scitotenv.2015.10.150.

References

Appelo, C.A.J., Postma, D., 2005. Geochemistry, Groundwater and Pollution. CRC Press.

Bauer, P., Langer, T., Prommer, H., Wolski, P., Kinzelbach, W., 2007. Okavango delta island: interaction between density-driven flow and geochemical reactions under evapoconcentration. J. Hydrol. 335, 389–405.

Biswas, A., Nath, B., Bhattacharya, P., Halder, D., Kundu, A.K., Mandal, U., et al., 2012. Hydrogeochemical contrast between brown and grey sand aquifers in shallow depth of Bengal basin: consequences for sustainable drinking water supply. Sci. Total Environ. 431, 402–412.

Buschmann, J., Berg, M., Stengel, C., Sampson, M.L., 2007. Arsenic and manganese contamination of drinking water resources in Cambodia: coincidence of risk areas with low relief topography. Environ. Sci. Technol. 41, 2146–2152.

Carpenter, R., 1969. Factor controlling the marine geochemistry of fluorine. Geochim. Cosmochim. Acta 33, 1153–1167.

Fang, L., 2006. Groundwater Monitoring Comprehensive Report From 2001 to 2005 in Baotou City, Inner Mongolia Geological Environment Monitoring (IMGEM) (In Chinese).

Guo, C., 1989. Bayan Obo Ore Deposit Geochemistry. Science Publishing House, Beijing (In Chinese).

Guo, W., Tong, K., 2011. Oppressive rare earth elements. Environ. Ecol. 6, 10–14 (In Chinese).

Guo, H., Zhang, B., Li, Y., Berner, Z., Tang, X., Norra, S., Stüben, D., 2011. Hydrogeological and biogeochemical constrains of arsenic mobilization in shallow aquifers from the Hetao basin, Inner Mongolia. Environ. Pollut. 159 (4), 876–883.

Han, D., Tong, X., Currell, M.J., Cao, G., Jin, M., Tong, C., 2014. Evaluation of the impact of an uncontrolled landfill on surrounding groundwater quality, Zhoukou, China. J. Geochem. Explor. 136, 24–39.

He, J., An, Y., Zhang, F., 2013. Geochemical characteristics and fluoride distribution in the groundwater of the Zhangye Basin in Northwestern China. J. Geochem. Explor. 135, 22–30.

Huang, X., 2011. China's rare earth resources efficient-clean extraction and recycling. In: Xiangshan (Fragrant Hills) Science Conference (Ed.)Frontiers and Future of Science (2009–2011). Science Press, Beijing (In Chinese).

Huang, X., Cao, G., Liu, J., Prommer, H., Zheng, C., 2014. Reactive transport modeling of thorium in a cloud computing environment. J. Geochem. Explor. 144, 63–73.

Hurst, C., 2010. China's Rare Earth Elements Industry:What Can theWest Learn? Institute for the Analysis of Global Security (IAGS), Washington, DC, p. 43

Jankowski, J., Acworth, R., Shekarforoush, S., 1998. Reverse ion-exchange in deeply weathered porphyritic dacite fractured aquifer system, Yass, New South Wales Australia. In: Arehart, G.B., Hulston, J.R. (Eds.), Proceedings of 9th international symposium on water–rock interaction, Taupo, New Zealand 30, pp. 243–246.

Johnson, D.B., Hallberg, K.B., 2005. Acid mine drainage remediation options: a review. Sci. Total Environ. 338, 3–14.

Ledesma-Ruiz, R., Pastén-Zapata, E., Parra, R., Harter, T., Mahlknecht, J., 2015. Investigation of the geochemical evolution of groundwater under agricultural land: a case study in northeastern Mexico. J. Hydrol. 521, 410–423.

Lghoul, M., Maqsoud, A., Hakkou, R., Kchikach, A., 2014. Hydrogeochemical behavior around the abandoned kettara mine site, morocco. J. Geochem. Explor. 144, 456–467.

Li, C., Gao, X., Wang, Y., 2015. Hydrogeochemistry of high-fluoride groundwater at yuncheng basin, northern China. Sci. Total Environ. 508, 155–165.

Liao, Z., 2013. Groundwater numerical simulation and regulation control in Baotou City (M.S. Thesis) China Institute of Water Resources and Hydropower Research (IWHR), Beijing, China (In Chinese with English abstract).

Liu, H., 2011. The situation of NORM in non-uranium mining in China. Presentation of the Dept. of Nuclear Safety Management, Ministry of Environment Protection, (National Nuclear Safety Administration) China.

Ma, P., 2012. Rare Earth Elements Reports. Metallurgical Industry Press, China (In Chinese).

Merchán, D., Auqué, L., Acero, P., Gimeno, M., Causapé, J., 2015. Geochemical processes controlling water salinization in an irrigated basin in Spain: identification of natural and anthropogenic influence. Sci. Total Environ. 502, 330–343.

Monjerezi, M., Vogt, R.D., Aagaard, P., Saka, J.D., 2011. Hydro-geochemical processes in an area with saline groundwater in lower Shire River valley, Malawi: an integrated application of hierarchical cluster and principal component analyses. Appl. Geochem. 26, 1399–1413.

Nie, Z., Ren, Y., Liu, Z., Du, C., Cong, P., 2011. Preliminary study on seismic active faults of the Daqingshan frontal fault in Baotou City, Inner Mongolia. Geoscience 25 (5), 938–957 (In Chinese with English abstract).

Olías, M., Nieto, J., Sarmiento, A., Cerón, J., Cánovas, C., 2004. Seasonal water quality variations in a river affected by acid mine drainage: the odiel river (South West Spain). Sci. Total Environ. 333, 267–281.

Pan, S.T., 2010. A study on the stability of Baogang tailings dam (M.S. Thesis) China University of Geosciences (Beijing), Beijing, China (In Chinese with English abstract).

Parkhurst, D.L., Appelo, C., 1999. User's Guide to PHREEQC (Version 2): A Computer Program for Speciation, Batch-reaction, One-dimensional Transport, and Inverse Geochemical Calculations.

Peeters, L., 2014. A background color scheme for piper plots to spatially visualize hydrochemical patterns. Groundwater 52 (1), 2–6.

Penman, A., 2001. Tailing dams—risk of dangerous occurrences. Int. Comm. Large Dams—Bull 121.

Shen, S., Liu, X., 1957. Neotectonism and its impacts on the geological and hydrogeological conditions in Baotou area. Hydrogeol. Eng. Geol. 8, 4–7 (In Chinese).

Shen, L., Luo, S., Zeng, X., Wang, H., 2011. Review on anti-seepage technology development of tailings pond in China. Procedia Engineering 26, 1803–1809.

Si, W., Liu, J., Cai, L., Jiang, H., Zheng, C., He, X., et al., 2015. Health risks of metals in contaminated farmland soils and spring wheat irrigated with yellow river water in Baotou, China. Bull. Environ. Contam. Toxicol. 94, 214–219.

Singh, A.K., Mondal, G., Singh, T., Singh, S., Tewary, B., Sinha, A., 2012. Hydrogeochemical processes and quality assessment of groundwater in dumka and jamtara districts, Jharkhand, India. Environ. Earth Sci. 67, 2175–2191.

Smedley, P.L., Zhang, M., Zhang, G., Luo, Z., 2003. Mobilisation of arsenic and other trace elements in fluviolacustrine aquifers of the Huhhot Basin, Inner Mongolia. Appl. Geochem. 18, 1453–1477.

Stumm, W., Morgan, J.J., 1995. Aquatic Chemistry: Chemical Equilibria and Rates in Natural Waters. John Wiley & Sons.

Thukral, A.K., 1989. Effect of tailings water irrigation on the biomass of some crop plants. J. Environ. Biol. 10 (4), 337–342.

Wang, X.L., 2006. Quaternary sedimentary and structure features of the hohholt-baotou basin, Inner Mongolia. China University of Geosciences (Beijing), Beijing, China, M.S. Thesis (In Chinese with English abstract).

Wang, Y., Tu, X., 1990. Percolating water's effect on quality of underground water and soil salinization from tailing pond of Baotou steel and iron company. Min. Geol. 11, 43–49 (In Chinese with English abstract).

Wolkersdorfer, C., 2008. Water Management at Abandoned Flooded Underground Mines: Fundamentals, Tracer Tests, Modelling, Water Treatment. Springer Science & Business Media.

Xie, X., Wang, Y., Li, J., Yu, Q., Wu, Y., Su, C., et al., 2015. Effect of irrigation on Fe (III)–SO_4^{2-} redox cycling and arsenic mobilization in shallow groundwater from the Datong basin, China: evidence from hydrochemical monitoring and modeling. J. Hydrol. 523, 128–138.

Xu, G., Shi, C., Wang, D., Zhao, Z., Wang, D., He, Z., et al., 2005. An emergency call for the protection of thorium and REEs resources at Bayan Obo and the prevention of radioactive contamination of the yellow river and Baotou. Bull. Chin. Acad. Sci. 20 (6), 448–450 (In Chinese).

Yang, K.-F., Fan, H.-R., Santosh, M., Hu, F.-F., Wang, K.-Y., 2011. Mesoproterozoic carbonatitic magmatism in the Bayan Obo deposit, Inner Mongolia, north China: constraints for the mechanism of super accumulation of rare earth elements. Ore Geol. Rev. 40, 122–131.

Yu, X.-L., Bai, L., Wang, Q.-C., Liu, J., Chi, M.-Y., Wang, Z.-C., 2012. Recovery of rare earths, niobium, and thorium from the tailings of giant Bayan Obo ore in China. Metall. Mater. Trans. B Process Metall. Mater. Process. Sci. 43, 485–493.

Zachara, J.M., Long, P.E., Bargar, J., Davis, J.A., Fox, P., Fredrickson, J.K., Freshley, M.D., Konopka, A.E., Liu, C., McKinley, J.P., Rockhold, M.L., Williams, K.H., Yabusaki, S.B., 2013. Persistence of uranium groundwater plumes: contrasting mechanisms at two DOE sites in the groundwater–river interaction zone. J. Contam. Hydrol. 147, 45–72.

Zhang, L., 2013. Summary on the dam-break of tailing pond. Shuili Xuebao 44 (5), 594–600 (In Chinese with English abstract).

Zheng, B., 1992. Research on Endemic Fluorosis and Industrial Fluoride Pollution. China Environmental Science Press, China (In Chinese).

Zheng, B., Lu, L., 1986. Using tritium tracing fluoride contamination of groundwater in Baotou area. Hydrogeol. Eng. Geol. 4, 35–37 (In Chinese).

Zhu, D., 1962. Comprehensive Report of Groundwater Monitoring and Hydraulic Dynamic Observation in Old-downtown Areas of Baotou City From 1956 to 1961. Hydrogeological Observation Station of the Inner Mongolia Bureau (In Chinese).